PROGRESS IN PHOTOVOLTAICS: RESEARCH AND APPLICATIONS
Prog. Photovolt: Res. Appl. 2008; **16**:679–685
Published online 24 July 2008 in Wiley InterScience (www.interscience.wiley.com) DOI: 10.1002/pip.848

Research *SHORT COMMUNICATION*

Imaging Physical Parameters of Pre-Breakdown Sites by Lock-in Thermography Techniques

O. Breitenstein*,†, J. Bauer, J.-M. Wagner and A. Lotnyk
Max Planck Institute of Microstructure Physics, Weinberg 2, D-06120 Halle, Germany

Local pre-breakdown sites in solar cells can be studied by lock-in thermography (LIT). Three new LIT techniques are proposed and demonstrated here, which are TC-DLIT for studying the local temperature coefficient of pre-breakdown sites, Slope-DLIT for measuring the normalized local slope of the I–V characteristics, and MF-ILIT for imaging the local carrier multiplication factor. First results on multi-crystalline silicon cells show that the pre-breakdown mechanism cannot completely be described by the conventional impact ionization and internal field emission models. Copyright © 2008 John Wiley & Sons, Ltd.

KEY WORDS: crystalline solar cells; pre-breakdown; lock-in thermography; internal field emission; impact ionization

Received 25 February 2008; Revised 23 June 2008

According to their net doping concentration of about $10^{16}\,cm^{-3}$, typical silicon solar cells should break down at a reverse bias above 50 V. However, at much lower reverse bias pre-breakdown may appear. For avoiding thermal destruction of solar modules by shading of single cells, the maximum allowed reverse current of typical solar cells is limited to some amperes at a reverse bias of 12–14 V. This criterion leads to the rejection of a non-negligible number of cells in the production line. The physical understanding of pre-breakdown processes is necessary in order to limit or avoid pre-breakdown by appropriate technological measures. Lock-in thermography (LIT) allows to image local heat sources in solar cells with a good spatial resolution.[1–3] Thus, it is an appropriate tool for investigating pre-breakdown sites. Figure 1 shows an electroluminescence (EL[4]) image of a multicrystalline mc-Si solar cell, which images grown-in recombinative crystal defects, together with two conventional lock-in thermography images measured in the dark (DLIT) at reverse biases of 11·5 and 14 V, respectively. Since only reverse bias LIT investigations are reported here, we will denote the reverse bias with positive numbers throughout this paper. All LIT images in this paper are measured at a lock-in frequency of 20 Hz. The comparison in Figure 1 shows a general correlation between grown-in defects and local pre-breakdown sites. However, as the circles show, there are some sites which are not at the position of recombinative crystal defects. These sites appear in our example only at 14 V but not yet at 11·5 V, hence they show a specially "hard" breakdown characteristic. Moreover, the edge of the cell, which was isolated by etching, also shows distinct pre-breakdown. Obviously there are different breakdown sites in this cell, which are based on several different physical mechanisms.

In the literature basically two mechanisms are discussed for breakdown in p–n junctions, which are impact ionization (avalanche effect) and internal field emission (Zener effect).[5–7] Impact ionization means that free carriers are accelerated by the electric field in the reverse-biased depletion region to such a high

* Correspondence to: O. Breitenstein, Max Planck Institute of Microstructure Physics, Weinberg 2, D-06120 Halle, Germany.
† E-mail: breiten@mpi-halle.mpg.de

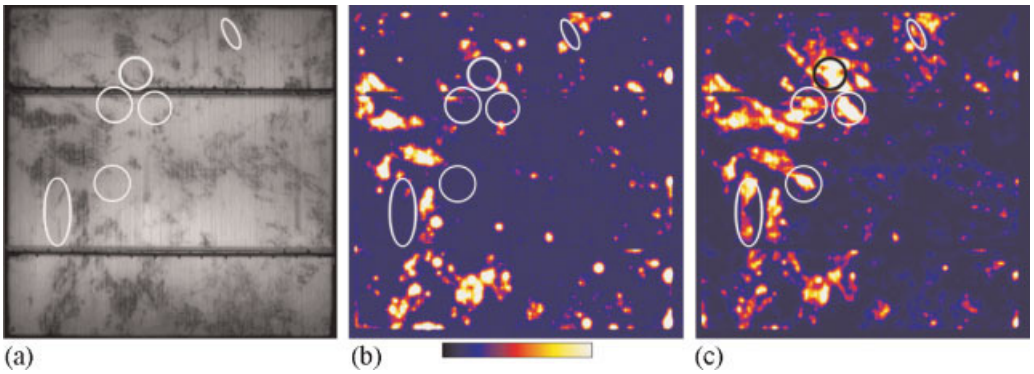

Figure 1. EL image (a), DLIT image at 11·5 V ($I = 0{\cdot}16$ A) reverse bias (b), and DLIT image at 14 V ($I = 1{\cdot}4$ A) reverse bias of a mc-Si solar cell, all taken at room temperature. In (b) one can see pre-breakdown sites, which correspond to the positions of defect regions in (a). The circles mark areas where good crystal quality is expected from (a), but in (c) in these positions hard breakdown occurs at higher reverse bias. The scale bar holds for (b) −0·5 to 5 mK and (c) −5 to 50 mK

energy that, at scattering events, they generate new electron–hole pairs. Internal field emission means that the electric field is so high that carriers may tunnel horizontally through the gap. These two mechanisms differ in their temperature coefficient. For impact ionization the breakdown current reduces with increasing temperature since the carriers are more strongly scattered at high temperature and may gain less kinetic energy. For internal field emission the current increases with temperature since the gap shrinks with increasing temperature. Multiplication of photo-induced carriers occurs only for impact ionization (avalanche effect), but not for internal field emission. For both mechanisms preferred breakdown in sites of crystal defects like dislocations has been reported.[5] However, a detailed theory for the influence of crystal defects on both mechanisms is still missing. Thus, the study of pre-breakdown phenomena in multicrystalline solar cells is an interesting field for studying this influence. Appropriate parameters for describing different breakdown mechanisms can be derived from the bias- and temperature-dependent dark local *I–V* characteristics and by characterizing the local carrier multiplication of photogenerated light.

In this work three new LIT techniques are proposed and tested to study relevant physical parameters of pre-breakdown sites. Two of them are special procedures to display a combination of two conventional LIT measurements, as it is done, e.g., for imaging the ideality factor or the saturation current density,[8] and one technique implies a special LIT measurement procedure, similar to R_s-ILIT.[2] It is well known that dark lock-in thermography (DLIT) results can be scaled in units of the flowing current density.[1,8] For this purpose the LIT signal which is −90° phase-shifted to the applied bias pulses has to be used, since only this signal is strictly additive and can be used as a measure of the locally dissipated power density.[1,8] Using the normally displayed amplitude signal would overestimate local (point-like) heat sources. Assuming that a whole cell with area A is imaged, the measured cell current is I, and the −90° LIT signal averaged across the whole image is $<T>$, the current density J in the position of a measured local LIT signal of magnitude T is

$$J = T\frac{I}{<T>A} \tag{1}$$

Two of the newly proposed techniques are based on a set of standard DLIT images taken at a number of different temperatures T_j and, for each temperature, at a number of different reverse biases V_i. For all these images the scaling procedure (1) has to be applied, leading to a two-dimensional set of two-dimensional current density images $J(x,y)_{i,j}$. Note that all these images must be taken with the same position of the cell in the image for ensuring a one-to-one correspondence of the pixel values. If, for a given bias V_i, two current density images of subsequent temperatures T_j and T_{j-1} are subtracted from each other and normalized to the average of these two images and the temperature difference, the result is an image which describes the temperature coefficient of the current between the temperatures T_j and T_{j-1} in the position of the breakdown sites. In accordance with the generally

DOI: 10.1002/pip

accepted nomenclature for different LIT techniques,[3] we propose to name this type of image ''Temperature-Coefficient-DLIT'' or ''TC-DLIT'' image:

$$\text{TC-DLIT} = \frac{2(J_{i,j} - J_{i,j-1})}{(T_j - T_{j-1})(J_{i,j} + J_{i,j-1})} \quad (2)$$

This image displays quantitatively the physically relevant magnitude of the relative temperature coefficient, which may be given e.g., in ''percent current change per K'' by multiplying (2) with 100. Note that this definition includes a normalization to the average current density and, therefore, effectively describes the slope of the current density at the midpoint T_{av} between T_j and T_{j-1} (central-difference derivative). This is in accordance with the assumption of a linear dependence underlying the approximation of the derivative by a difference quotient, which for a nonlinear dependence is only correct if the measured values are lying sufficiently close together.

The TC-DLIT image easily allows to distinguish between breakdown sites with positive and those with negative temperature coefficient of the current, and also between different values of the temperature coefficient, independent of the magnitude of the breakdown current. Outside of breakdown sites, or in grid regions or regions outside the cell, this image shows essentially noise (as does also the phase image[1]). In these regions, the image values may be blanked artificially to zero.

In the same way, for a given temperature T_j, two current density images of subsequent biases V_i and V_{i-1} may be subtracted from each other and normalized to the average of both and the bias difference. The result is an image which quantitatively describes the relative slope of the I–V characteristics of all breakdown sites. The unit is V^{-1}; a local value of $1\ \text{V}^{-1}$ means that the local current density changes by $100\%\ \text{V}^{-1}$, referred to the average current density expected for the average bias V_{av}. We propose to name this type of image ''Slope-DLIT'' image:

$$\text{Slope-DLIT} = \frac{2(J_{i,j} - J_{i-1,j})}{(V_i - V_{i-1})(J_{i,j} + J_{i-1,j})} \quad (3)$$

This image allows to distinguish between breakdown sites of different steepness of the I–V characteristic, which are traditionally called ''soft'' or ''hard'' breakdowns,[7] independent of their magnitude. It shows noise outside of breakdown sites, as the TC-DLIT image does, which may be blanked artificially to zero on demand.

Note that if the smaller of the two current density values is negligible against the larger one, the results based on (2) and (3) approach the limits $2/(T_j - T_{j-1})$ and $2/(V_i - V_{i-1})$, respectively, and do not further increase with increasing current difference. This is due to the fact that, in this case, the reference current density used for normalization increases proportionally to the absolute slope of the current density at that point, so the relative slope remains independent of the absolute slope. This is physically correct as long as the linear approximation is valid. However, especially for bias-dependent measurements, we may have a strong, nonlinear onset of the current between the two measurement points. In this case the relative slope always equals $2/(V_i - V_{i-1})$, which therefore should be interpreted as an indication of the necessity to repeat the measurement with a smaller bias increase.

The absolute slope of the local breakdown current may also be directly measured by a special ''differential'' DLIT technique, which was already proposed for forward bias imaging by Kaes *et al*.[9] Here the bias is not pulsed from zero to a certain voltage V but is square-shape modulated between V_1 and V_2, with V_2 being close to V_1. Also this image can be scaled quantitatively, but here the magnitude of the breakdown current still influences the signal. Hence, a strong breakdown site with a weak slope is displayed in the same brightness as a weak breakdown site with a high slope. Nevertheless, we will include such an example for comparison below.

Finally, for studying avalanche effects, it is useful to image the local value of the carrier multiplication factor. The multiplication factor is defined as the ratio of a photocurrent at a given voltage to its constant value at small values of the reverse bias.[6] The special procedure proposed here is to perform LIT at a constant (not pulsed) reverse bias with a pulsed homogeneous illumination of the cell. The light intensity may be as weak as 0·1 sun. Since the photocurrent due to this optical excitation (wavelength 850 nm in our case) is essentially homogeneous for a reasonably good solar cell, at low reverse bias we expect an essentially homogeneous -90° image of the cell. Note that under this measurement condition the dominant pulsed heat source is the thermalization of the photocurrent across the reverse-biased p–n junction. If in a certain position avalanche multiplication takes place, this region will appear brighter than its surrounding. For obtaining quantitative results, and for correcting any inhomo-

DOI: 10.1002/pip

geneities of the photocurrent, we propose to divide such a photocurrent density image taken at the desired voltage V by a second one taken at a sufficiently low voltage V_{low}, where no avalanche multiplication appears throughout the cell. Note that for this technique we cannot use (1) for converting the LIT images (given in mK T-modulation) into current density images because the measured current is the sum of the constant dark current (already containing pre-breakdown currents) and the pulsed photocurrent. Instead, here we use a technique which was already used in the so-called LIVT technique (local I–V characteristics measured thermally).[10] There a value proportional to the current was obtained from the thermal signal by dividing it through the applied bias V. In our case, the energy dissipated by the photogenerated electrons is the current density multiplied by the sum of the applied voltage V, the diffusion voltage V_D (about 0·95 V for typical solar cells) and the thermalization voltage for the photogeneration V_{th}, which is about $(h\nu - E_g)/e = 0{\cdot}35$ V for 850 nm light. Thus, the final procedure for imaging the multiplication factor is:

$$\text{MF-ILIT} = \frac{(V_{low} + V_D + V_{th})\,T(V)}{(V + V_D + V_{th})\,T(V_{low})} \qquad (4)$$

We propose to name this image "Multiplication-Factor-ILIT" or "MF-ILIT" image. The data of this image are unity in regions without any carrier multiplication and correspondingly higher if multiplication takes place.

Figures 2–4 show first results of the above proposed LIT techniques for the sample already imaged in Figure 1. In Figure 2, a TC-DLIT image calculated by applying (2) to two DLIT images of the sample of Figure 1 measured at a reverse bias of 13 V at 40 and 60°C is shown in two different scaling ranges. These images display the temperature coefficient of the breakdown sites visible in Figure 1(b) at $T_{av} = 50$°C. The dark areas correspond to negative and the bright areas to positive TCs, respectively. For avoiding the disturbing noise and for showing a well-defined zero value, all regions in these figures where $(J_{i,j} + J_{i,j-1})$ was below a certain threshold value have been artificially blanked to zero. Figure 2(a), which is scaled between −3 %/K and +3 %/K, shows that the etched edge, and also two spots in the area (see circles in Fig. 2(b)), show a clearly positive TC. The bright outer edge of most regions is probably an artifact of the measurement coming from a T-dependent lateral heat diffusion, the "real" TC is always that at the breakdown sites. There are some regions with a clearly negative TC, but most breakdown regions show a low TC. Figure 2(b), which is scaled more sensitively between −1 %/K and +1 %/K, shows that most of the latter regions show a slightly negative TC (about −0·3 %/K); only some of them show a TC between ±0·05 %/K. Hence, according to their TC, at least four different classes of breakdowns can be

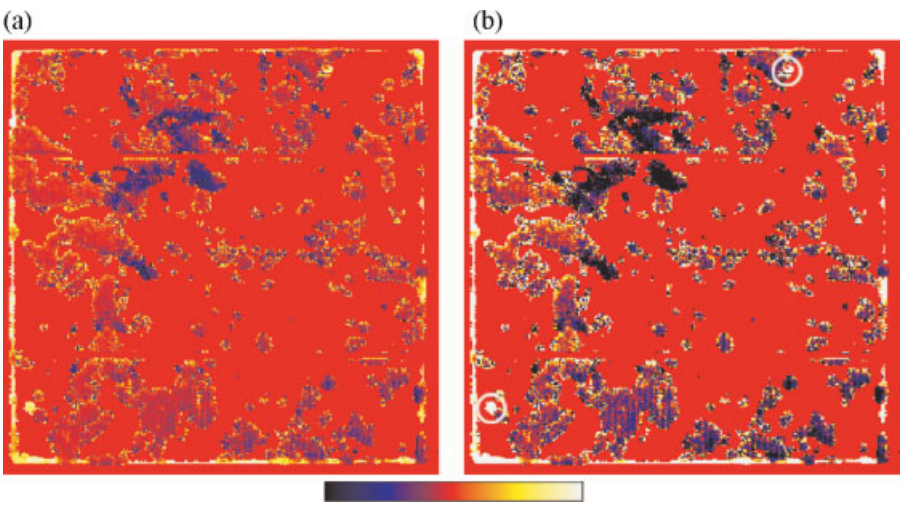

Figure 2. TC-DLIT image using DLIT images taken at 13 V and $T_1 = 40$°C and $T_2 = 60$°C ($T_{av} = 50$°C). The scaling in (a) is from −3 to 3 %/K and in (b) from −1 to 1 %/K. The noisy regions are blanked to zero

DOI: 10.1002/pip

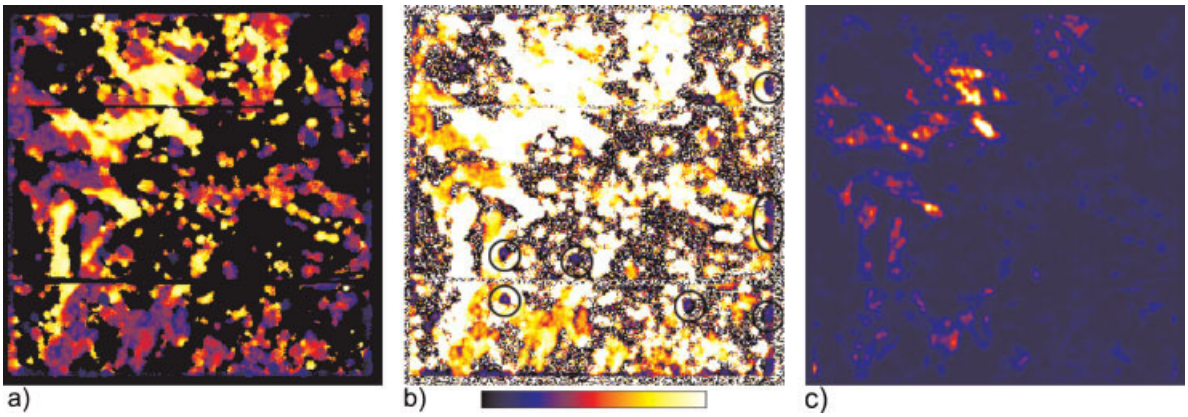

Figure 3. Slope-DLIT (a, b) and differential DLIT image (c). For (a, b) DLIT images taken at $T = 60°C$, $V_1 = 13$ V, and $V_2 = 14$ V were used ($V_{av} = 13{\cdot}5$ V). In (a) the noise was blanked to zero and the scaling is from 0 to 2 V^{-1}. In (b) the same image without noise blanking is shown in order to see sites with a slope <1 V^{-1} more clearly (marked by circles) and the scaling is from 0 to 1 V^{-1}. Also (c) was measured at $T = 60°C$, $V_1 = 13$ V, and $V_2 = 14$ V ($V_{av} = 13{\cdot}5$ V), the scaling range is from -2 to 20 mK

distinguished, those with strongly positive, with strongly negative, with slightly negative, and with nearly zero TC. Note that in these images, as well as in Figure 3, the exact position of the breakdown sites is hardly visible. Instead, they appear as extended regions of constant brightness. This is due to the fact that the whole halo region around the heat sources, which appears in LIT due to the lateral heat diffusion in the silicon material,[1] contains the information evaluated by (2) and (3). Only due to this property well-defined parameters can be measured for local heat sources in spite of the thermal blurring. Note that in this example with $(T_j - T_{j-1}) = 20$ K the data values of ± 3 %/K lie well below the above-mentioned limit of $2/(T_j - T_{j-1}) = 0{\cdot}1$/K, i.e., 10 %/K.

Figure 3 shows a Slope-DLIT and a ''differential'' DLIT image of this cell.[9] Images (a) and (b) are constructed from DLIT images measured at 60°C at $V_1 = 13$ V and $V_2 = 14$ V by applying (3), again displayed in two different scaling ranges. These images display the relative (normalized) *I–V* slope of the characteristics of the breakdown sites visible in Figure 1 at $V_{av} = 13{\cdot}5$ V. In Figure 3(a), by setting a threshold value for $(J_{i,j} + J_{i-1,j})$, the noisy regions outside of breakdown sites have been artificially set to zero. By comparing figures, Figure 1(b) and Figure 1(c), it was already visible that by increasing the reverse bias from 11·5 to 14 V, many new breakdown sites appear in the cell. As expected, the brightest areas in Figure 3(a), which show a slope up to 2 V^{-1}, contain the areas marked by the circles in Figure 1. However, considerably more regions appear so bright in this image. This is because (3) works independent of the magnitude of a breakdown site. So also weak breakdown sites showing a high slope appear bright in Figure 3(a). As mentioned above, this value of 2 V^{-1} equals the limit for the relative slope (for $V_i - V_{i-1} = 1$ V), hence it is very likely that in this case we have a sudden onset of the current between the two bias values. Most of the other breakdown sites show a slope between 0·5 and 1 V^{-1}, which is smaller than this limit. In Figure 3(b), which is scaled more sensitively than (a), the noise canceling procedure was not applied. This image shows some dark regions with a value of about 0·2 V^{-1} (see circles, including most of the edge region), which can be attributed to breakdown sites in Figure 1. They obviously represent an own class of pre-breakdown sites with especially soft breakdown. Figure 3(c) shows for comparison a ''differential'' DLIT image of the absolute slope according to Kaes *et al.*,[9] which has been measured also at 60°C by modulating the bias between $V_1 = 13$ V and $V_2 = 14$ V. As expected, this image shows the ''hard'' breakdown sites with high intensity marked in Figure 1 as the dominating ones, but it does not allow to distinguish between weak hard and strong soft breakdowns.

The MF-ILIT procedure described above (keeping the reverse bias constant and pulsing a homogeneous illumination, here about 0·1 sun intensity) has been applied to this sample for various values of the reverse bias. It turned out that up to 13 V the LIT images measured in this way appeared essentially homogeneous, as expected if no avalanche multiplication

DOI: 10.1002/pip

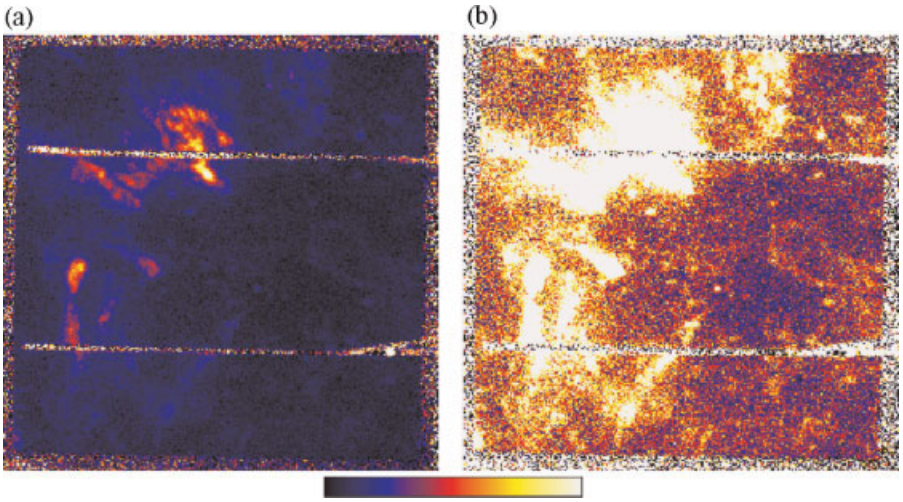

Figure 4. MF-ILIT image of the solar cell measured at room temperature using $V_{low} = 13$ V and $V = 15$ V. The scaling in (a) is from 1 to 4 and in (b) from 1 to 1·5

takes place. So 13 V has been used as "V_{low}" in (4). Figure 4 shows an MF-ILIT image according to (4) measured at room temperature at $V = 15$ V, again displayed in two scaling ranges. Figure 4(a) shows that at 15 V reverse bias the multiplication factor in some regions reaches a value of 4. These are the regions of hard breakdown, which were marked in Figure 1. Figure 4(b) shows that there are many other local regions with a weaker multiplication factor in the order of 1·3. It seems that all breakdown sites show at 15 V at least a weak avalanche multiplication. Even in regions without breakdown sites the MF at 15 V is about 1.1.

Already these preliminary results show that pre-breakdown sites cannot be completely described by the well-known avalanche- and internal field emission theory. As expected for avalanche breakdown, the regions with the steepest breakdown also show the highest avalanche multiplication factor and a clearly negative TC, and in regions with positive TC there is no avalanche multiplication. However, the negative TC occurs already at a reverse bias of 13 V and below, where already pre-breakdown occurs, but definitely no avalanche multiplication can be observed yet. Moreover, there are also regions with avalanche multiplication at higher bias, which show nearly zero TC. We have no explanation yet for the observed very low slope breakdown sites. So further experimental and theoretical work is needed for a better understanding of defect-induced pre-breakdown.

The LIT techniques proposed here facilitate the quantitative imaging of physically relevant parameters of pre-breakdown sites such as the temperature coefficient of the breakdown current, its normalized slope, and the local avalanche multiplication factor. For obtaining meaningful results, the temperatures and bias voltages used in (2) and (3) should be chosen sufficiently close together. Reliably measuring these parameters for different pre-breakdown sites is the presupposition to distinguish them from each other for studying their physical origin. Thus, the family of special LIT techniques for investigating solar cells [2, 3, 8, 9, 10] is extended now by the new members TC-DLIT, Slope-DLIT, and MF-ILIT.

Acknowledgements

This work was supported by the BMU project 0327650D (SolarFocus). The EL image Figure 1(a) was kindly provided by ISFH (Hameln). The help of Q-Cells AG (Thalheim) in supplying the cells used in this investigation is acknowledged.

REFERENCES

1. Breitenstein O, Langenkamp M. *Lock-in Thermography: Basics and Use for Functional Diagnostics of Electronic Components*. Springer: Berlin, 2003; ISBN 3-540-43439-9.
2. Breitenstein O, Rakotoniaina JP, van der Heide ASH, Carstensen J. Series resistance imaging in solar cells by lock-in thermography. *Progress in Photovoltaics: Research and Applications* 2005; **13**: 645–660, DOI: 10.1002/pip.623.

3. Breitenstein O, Rakotoniaina JP, Kaes M, Seren S, Pernau T, Hahn G, Warta W, Isenberg J. Lock-in thermography—A universal tool for local analysis of solar cells. *Proceedings of the 20th European Photovoltaic Solar Energy Conference and Exhibition,* Barcelona, 6–10 June, 2005; 590–593.
4. Fuyuki T, Kondo H, Yamazaki T, Takahashi Y, Uraoka Y. Photographic surveying of minority carrier diffusion length in polycrystalline solar cells by electroluminescence. *Applied Physics Letters* 2006; **86**: 262108. DOI: 10.1063/1.1978979.
5. Chynoweth AG, Pearson GL. Effect of dislocations on breakdown in silicon p–n junctions. *Journal of Applied Physics 1958*; **29**: 1103–1110. DOI: 10.1063/1.1723368.
6. Chynoweth AG, McKay KG. Internal field emission in silicon p–n junctions. *Physical Review* 1957; **106**: 418–426. DOI: 10.1103/PhysRev.106.418.
7. Mahadevan S, Hardas SM, Suryan G. Electrical breakdown in semiconductors. *Physica Status Solidi (a)* 1971; **8**: 335–374.
8. Breitenstein O, Rakotoniaina JP, Al Rifai MH. Quantitative evaluation of shunts in solar cells by lock-in thermography. *Progress in Photovoltaics: Research and Applications* 2003; **11**: 515–526. DOI: 10.1002/pip.520.
9. Kaes M, Seren S, Pernau T, Hahn G. Light-modulated lock-in thermography for photosensitive pn-structures and solar cells. *Progress in Photovoltaics: Research and Applications* 2004; **12**: 355–363. DOI: 10.1002/pip.555.
10. Konovalov I, Breitenstein O, Iwig K. Local current-voltage curves measured thermally (LIVT): a new technique of characterizing PV cells. *Solar Energy Materials and Solar Cells* 1997; **48**: 53–60. DOI: 10.1016/S0927-0248(97)00069-X.